

# MICE Target Simulation

Tom Lord, Paolo Franchini

June 5, 2018

## Contents

|  |          |
|--|----------|
| <b>1 Motivation</b>                              | <b>2</b> |
| <b>2 The MICE target in the ISIS proton beam</b> | <b>2</b> |
| <b>3 MARS simulation</b>                         | <b>2</b> |
| <b>4 MAUS simulation</b>                         | <b>5</b> |
| 4.1 Monte Carlo and data comparison . . . . .    | 6        |
| <b>5 Luminosity monitor</b>                      | <b>6</b> |
| <b>6 Conclusions</b>                             | <b>6</b> |
| <b>Appendices</b>                                | <b>8</b> |

## Abstract

Simulation of the pion production coming out from the MICE target using the MARS simulation software and implementation of this simulation into the MICE Monte Carlo software.

## 1 Motivation

Non trivial discrepancies in the data versus Monte Carlo comparison have justified the necessity to reconsider the pions momentum distribution used as primary input of the MICE Monte Carlo. The former model consisted in a fit done with three Gaussian of a pion distribution produced in 2008 with a earlier version of the MARS simulation software. Lack of documentation on this first study made hard to evaluate the goodness of the model that shows a peculiar hard cut in the distribution.

The MICE target has been described in its major components using the MARS simulation software.

## 2 The MICE target in the ISIS proton beam

The MICE target operates parasitically on protons undergoing acceleration within the ISIS synchrotron, dipping into the low-density halo of the beam on selected pulses just prior to their extraction, with an 1 Hz frequency. It is designed as a bored TiAl cylinder with inner radius 2.275 cm and outer radius 2.975 cm. The resulting thickness of material for proton collisions is significantly lower than one interaction length, giving an approximate interaction probability of  $x \times$ . As a result of this, very large numbers of protons on target are required for sufficient statistics.

The ISIS synchrotron circulates two beam bunches of approximately  $1.4E13$  protons each per cycle, with these undergoing close to 10,000 revolutions before extraction in a circulation time of 10ms. Proton beam-size shrinking between radii of 67mm and 48mm during it's acceleration through the synchrotron means proton collision energy and beamwidth will both vary in time with respect to the initial ISIS proton injection trigger, as well as due to small field fluctuations. Hence the target undergoes many proton collisions of between 650MeV and 800MeV collision energy during each dip.

Furthermore due to the field changes in the synchrotron, the ISIS beam often drifts from the well-defined beam center, such that the beam centre displacement (BCD) figure recorded is only a nominal value.

As noted in [4] the target is operated through the RATS control software, allowing the user to alter both BCD and User Delay (defined from the machine start trigger +  $(2^n \times 20ms) - 15ms$ , with n some integer) s.t. dips travelling further to achieve lower BCD may operate with reduced User Delay to compensate.

## 3 MARS simulation

The design of the MICE target, in particular the surrounding structure, is defined as in Fig. ???. The presented design has been based on schematics (ref) and surveys (refs). The MICE beamline is orientated at 25 deg with respect to the ISIS

| Time after injection (ms) | Proton Energy (MeV) |
|---------------------------|---------------------|
| 7.0                       | 615.59              |
| 7.1                       | 626.53              |
| 7.2                       | 637.25              |
| 7.3                       | 647.73              |
| 7.4                       | 657.96              |
| 7.5                       | 667.93              |
| 7.6                       | 688.62              |
| 7.9                       | 687.02              |
| 7.8                       | 696.12              |
| 7.9                       | 704.90              |
| 8.0                       | 713.35              |
| 8.1                       | 721.47              |
| 8.2                       | 729.23              |
| 8.3                       | 736.64              |
| 8.4                       | 743.68              |
| 8.5                       | 750.33              |
| 8.6                       | 756.60              |
| 8.7                       | 762.48              |
| 8.8                       | 767.95              |
| 8.9                       | 773.01              |
| 9.0                       | 777.65              |
| 9.1                       | 781.87              |
| 9.2                       | 785.66              |
| 9.3                       | 789.02              |
| 9.4                       | 791.94              |
| 9.5                       | 794.41              |
| 9.6                       | 796.44              |
| 9.7                       | 798.02              |
| 9.8                       | 799.15              |
| 9.9                       | 799.83              |
| 10.0                      | 800.06              |

Table 1: Time after injection (ms) vs Proton Energy in the ISIS beam (MeV). Interactions from target dipping occur over this time range.

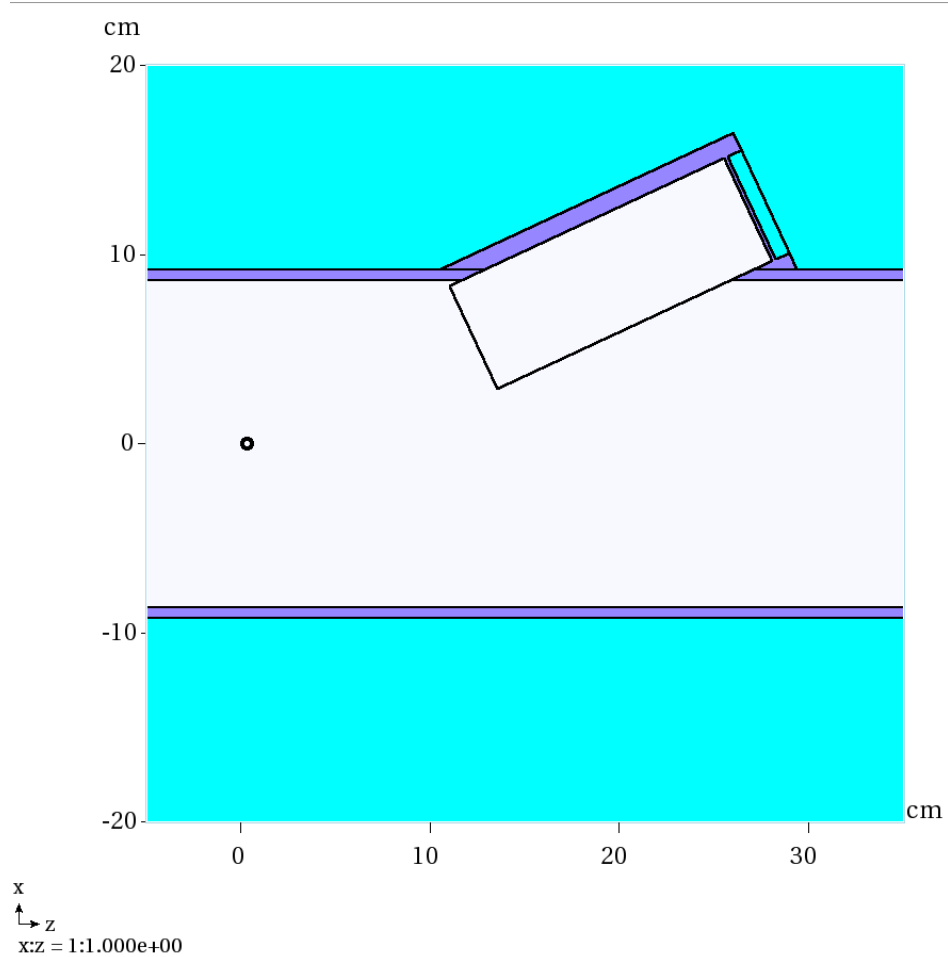


Figure 1: Design of the target in the MARS simulation. ( require  $z=60\text{cm}$ ?along the x-axis? )

beamline section where the target is located. In addition to the cylindrical bored-target structure from the previous model, various features of the surrounding ISIS beampipe structure have been included, such as the rectangular beampipe shape and target window structure, similarly oriented at 25 degrees toward the MICE beamline. The resulting pion distribution is collected as the particle flux through a surface downstream between the ISIS and MICE beamlines.

As both BCD and User Delay are altered live by the MICE operator to respond to ISIS beam drift & target deterioration in order to optimise statistics, modelling of an exact dip cycle to replicate that throughout the entire MICE data collection is difficult. Instead a number of model iterations with varying proton energy and beamwidth have been simulated to compare pion production, momentum distribution & results from downstream propagation.

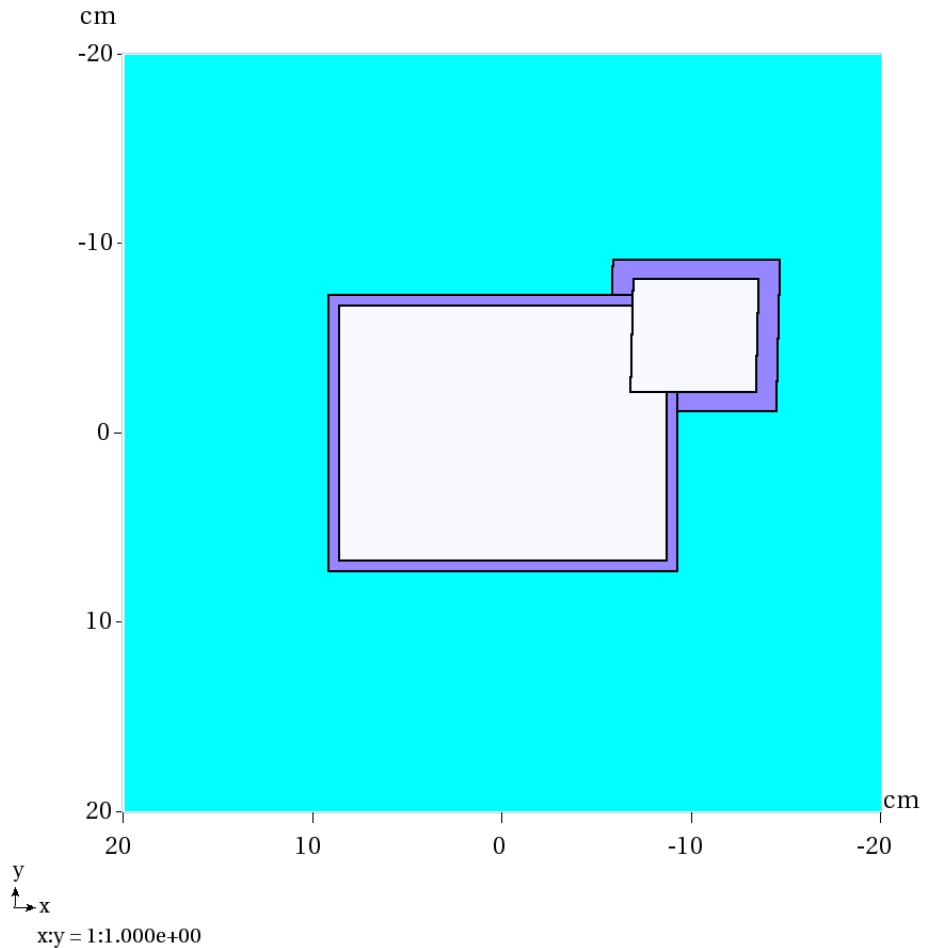


Figure 2: Design of the target in the MARS simulation. ( require  $z=60\text{cm}$ ?along the x-axis? )

## 4 MAUS simulation

The Monte Carlo in MICE is produced in a two-step process. In the first step a pion beam is produced according to an initial momentum distribution and is propagated using G4BL up to the bending dipole D2. After this point MAUS takes over propagating the particles (pions, muons and electrons coming from decays) through the remaining part of the beamline up to the EMR, passing through the cooling channel, according to the geometry and run selected to be simulated.

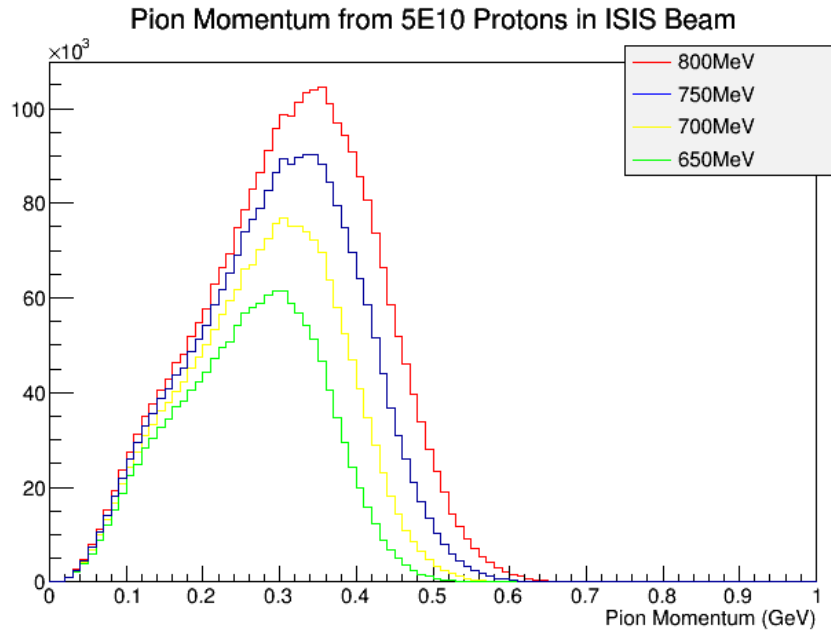


Figure 3: Hist needs updating with new models statistics

#### 4.1 Monte Carlo and data comparison

A few figures of merit have been considered: time of flight of the particles between TOF0 and TOF1 and momentum distribution of pions and muons in the upstream tracker at station 5. Simulations have been produced for 140, 200 and 240 MeV/c nominal pionic beams, with further

### 5 Luminosity monitor

A luminosity monitor (Fig. 4, 5) has been designed and constructed to measure the particle rate close to the MICE target and determine the number of protons hitting the target as a function of depth.

### 6 Conclusions

### References

- [1] <https://mars.fnal.gov/>
- [2] MICE note #216, <http://mice.iit.edu/micenotes/public/pdf/MICE0216/MICE0216.pdf>
- [3] MICE note #242, <http://mice.iit.edu/micenotes/public/pdf/MICE0242/MICE0242.pdf>

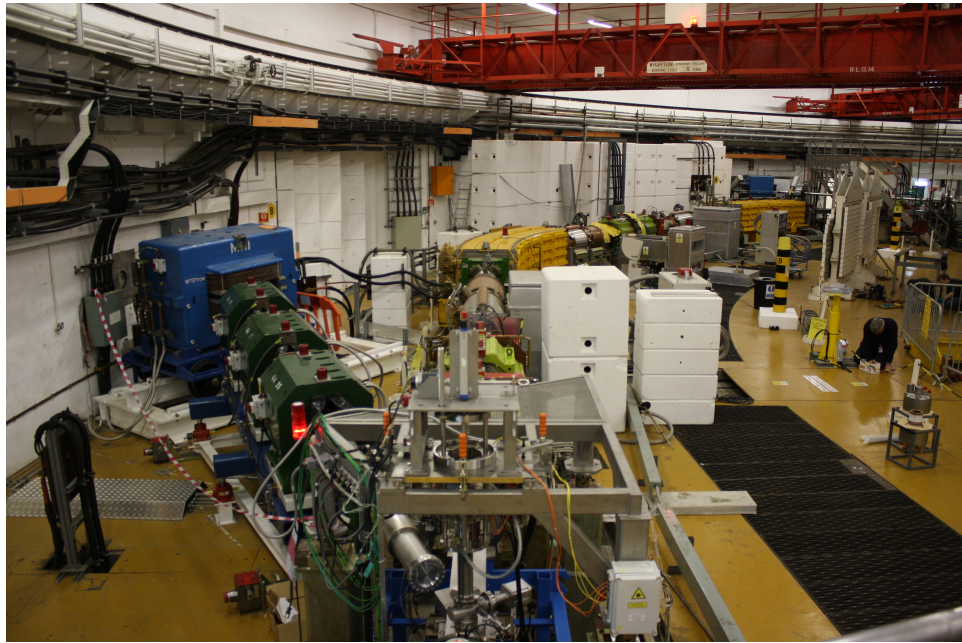


Figure 4: View of the ISIS synchrotron from above the targeted. MICE beam line on the left and luminosity monitor on the right 10 m away, standing on the top of the yellow turret.

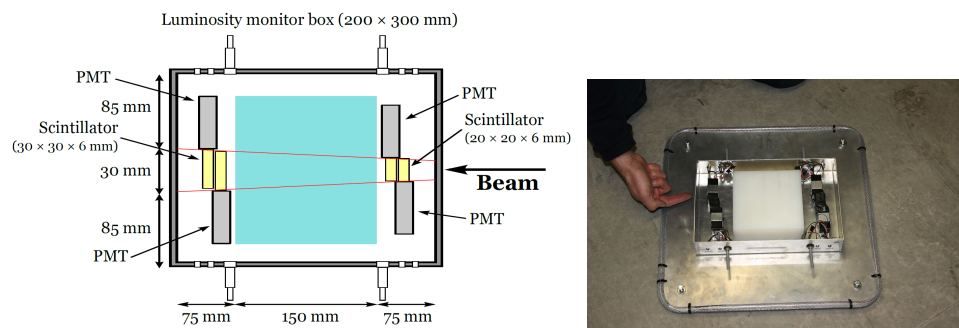


Figure 5: Design of the luminosity monitor (left) and the luminosity monitor box itself (right).

- [4] MICE note #480, <http://mice.iit.edu/micenotes/public/pdf/MICE0480/MICE0480.pdf>
- [5] ISIS Survey Drawing 1-SI-6305-031-01-D, M113 Vacuum Vessel
- [6] ISIS Survey Drawing 1-SI-6305-031-02-C, M113 Vacuum Vessel
- [7] ISIS Survey Drawing 1-SI-6305-031-03-C, M113 Vacuum Vessel
- [8] ISIS Survey Drawing 0-SI-5100-105-04-I, Essential Geometry of ISIS

## Appendices

ISIS Survey Drawing

